A Novel Response-Translating Lowpass Filter Achieving 1.4-to-15-Hz Tunable Cutoff for Biopotential Acquisition Systems

Chon-Teng Ma, Pui-In Mak, Mang-I Vai, Peng-Un Mak, Sio-Hang Pun, Wan Feng and R. P. Martins [1]

Biomedical Engineering and Analog and Mixed-Signal VLSI Laboratories, FST,
University of Macau, Macao, China (E-mail: ma86547@umac.mo)
1 — On leave from Instituto Superior Técnico (IST)/UTL, Lisbon, Portugal

ABSTRACT

This paper presents a response-translation technique to realize an ultra-low-cutoff lowpass filter in small area for biopotential acquisition systems. It is by exploiting a chopper-stabilized instrumentation amplifier (IA) with *bandpass* characteristic to obtain a *lowpass* response after chopper stabilization, resulting in substantial area savings because of relaxed time constant in the implementation. Optimized in a 90-nm CMOS process with 2.5-V thick-oxide devices, a 2nd-order OTA-C ladder filter demonstrates –40 dB/decade stopband attenuation, 1.4-15 Hz frequency tunability, and strong relaxation of the required time constant (depends on the set chopper frequency). The entire lowpass filter draws 8.37 µA at a 3-V supply.

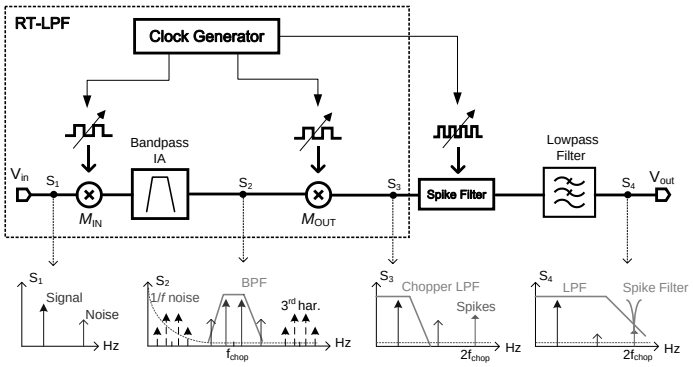

Fig. 1. Operating principle of the proposed RT-LPF.

1. INTRODUCTION

Low-pass filters are crucial building blocks for wearable biomedical devices. The amplitudes of the biopotential signals are in the order of tens of μV to tens of mV and the frequency span from DC to a few kHz. Among such a wide frequency range, low-frequency bands selection (1–10 Hz) is very critical for obtaining a particular content such as the well-known electroencephalograph (EEG) waves: δ (1–4 Hz), θ (4–8 Hz), α (8–13 Hz). Unfortunately, filter with a very low cutoff cannot be designed in a simple manner as the fabrication cost of the chip will be increased when large time constants are required for integrated circuit implementation. The state-of-the-art [1-3] reduces the silicon area by applying different circuit structures for achieving an ultra low transconductance. Yet, lowering the transconductance leads to substantial noise increment. Further, due to the low-frequency characteristic and µV level of bio-potential signals, the 1/*f* noise of the measuring devices must be concerned.

In order to acquire, area-efficiently, the weak biopotential signals using an ultra-low-cutoff lowpass filter while achieving low passband noise, a response-translating lowpass filter (RT-LPF) is proposed. It re-uses the choppers and the bandpass characteristic of the IA for response translation, i.e., convert a high-frequency reasonable Q bandpass filter into a lowpass filter with a small cutoff, resulting in significant area reduction due to the relaxed time constant. The chopper stabilization [4] still maintains its advantage of 1/*f* noise filtering. The bandpass IA here is a 2nd-order operational transconductance amplifier-capacitor (OTA-C) ladder filter. The OTA is based on the Nauta cell that involves only CMOS inverters and is suitable to realize a high-Q bandpass response with small power and area.

2. ARCHITECTURE OF THE CLF

Figure 1 shows the operating principle of the proposed RT-LPF, which consists of a bandpass IA with input and output choppers. A spike filter and a backend lowpass filter can be added to suppress the modulated noise and spikes. A tunable clock generator offers the modulation signals to the choppers and the spike filter. The input chopper modulator (M_{IN}) will first frequency-translate the input biopotential signal and the corresponding contaminating signals from spectrum S_1 to S_2. The chopper frequency (f_{chop}) should be much larger than the 1/*f* noise corner frequency of the IA, to minimize the noise contribution of the choppers to the total output noise power spectral density (PSD). Thus, f_{chop} is fixed in a range of few kHz. As depicted in spectrum S_2, the input signal of the IA is split into the upper and lower sidebands. The bandpass characteristic of the IA with a center frequency equals to f_{chop} will select the desired signal, while rejecting the unwanted interferers, noise and odd-harmonic components at the high frequency bands. As a result, the time constant for the implementation of the bandpass filter can be much relaxed and the 1/*f* noise of the IA can be suppressed at the same time. Finally, the output chopper modulator (M_{OUT}) will frequency-translate both the signal and noise back to the baseband (spectrum S_3).

As usual, spikes are generated after chopping, due to the charge injection associated with the switches of the chopper. These spikes can be easily eliminated by applying a track-and-hold-like spikes filter [5] and a simple backend lowpass filter which are not included in this work. The expected final response after frontend and backend lowpass filtering is shown in spectrum S_4.

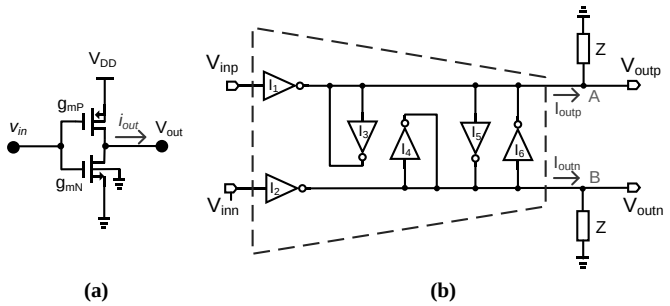

(a) **(b)**

Fig. 2. (a) CMOS inverter and (b) Nauta-cell-based OTA.

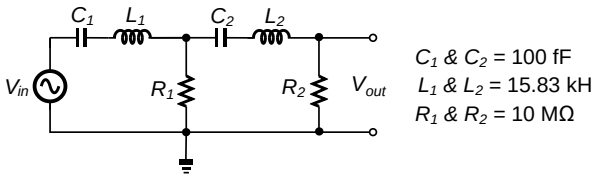

Fig. 3. Modified *RLC* ladder equivalent circuit of a 2nd-order bandpass filter.

3. CMOS-INVERTER-BASED OTA

OTA-C is a common topology for continuous-time filters. In this work, the Nauta cell [6] is used as the OTA which involves only simple CMOS inverters while requiring no common-mode feedback circuit and is directly self voltage biased. Figure 2(a) shows the schematic of a typical CMOS inverter. When the PMOS and NMOS transistors are in the saturation region, the inverter's transconductance (g_m) is given by,

$$g_m \approx r\xi_P(V_{DD} - \frac{|V_{tp}|}{2})^{r-1} + u\xi_N(V_{DD} - \frac{|V_{tn}|}{2})^{u-1} \quad , \qquad (1)$$

where ξ_N and ξ_N are process dependent parameters depending on the field-oxide depth, transistor's size and mobility. In addition, for a quadratic behavior of the MOS transistors, r and u are equal to 2. Thus, assuming that the input common-mode voltage V_{CM} is half of the supply $V_{DD}/2$, g_m can be simplified to the sum of the PMOS and NMOS gate-source transconductance, i.e. $g_m = g_{mP} + g_{mN}$.

A Nauta cell with a ground load impedance Z is shown in Fig. 2(b). With no parasitic pole the Nauta cell was originally proposed for high-frequency filtering. Here, it is also suitable for implementing a bandpass filter with a high Q under a very small bias current. Besides, it also avoids the need of common-mode feedback circuit. This is because when node **A** and **B** are directly shorted to the ground, the output current I_{outp} and I_{outn} are controlled by the input voltage V_{inp} and V_{inn}. This characteristic can be found from the general expression of the current-to-voltage transfer function of the Nauta cell as given by,

$$I_{outp} = \frac{g_m}{2}(V_{inp} - V_{inn}) + \frac{g_m}{1+2g_mZ}\frac{(V_{inp} - V_{inn})}{2} \quad . \qquad (2)$$

When the inverter's output conductance (g_d) is taken into account, we obtain $Z = Z' / (Z' + 3\ g_d)$. According to (2), the common-mode gain (G_{CM}) can be simplified to be $g_m/2$ when Z is high enough. Thus G_{CM} will be independent to the load impedance. One of the best solutions for attaining a higher Z is by adding buffers at the output of the OTA.

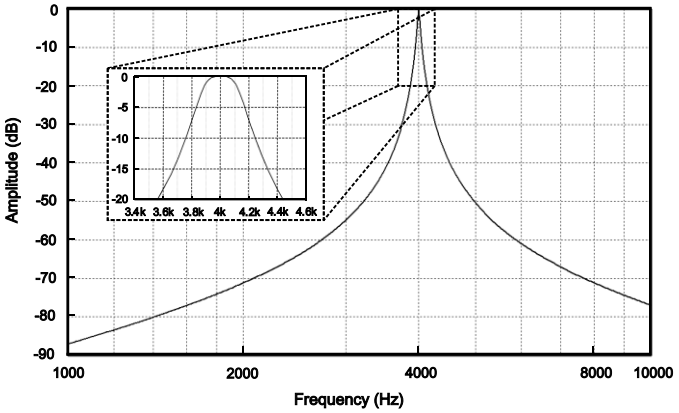

Fig. 4. Frequency response of Fig. 3 with a center frequency of 4 kHz.

4. RESPONSE-TRANSLATING LOWPASS FILTER (RT-LPF)

A. Filter Synthesis

Ladder-type filter is superior for high-order filtering because of its low sensitivity to component variation, especially in their passband. Though a typical passive ladder-type bandpass filter can be easily deducted with the help of the filter handbook, it requires large grounding capacitors or inductors that are not easy to be realized by active devices. Therefore, a 2nd-order *RLC* ladder filter is proposed as shown in Fig. 3, which is customized from a 3rd-order Butterworth bandpass filter by removing the central grounding *LC* circuit. The corresponding simulated frequency response is shown in Fig. 4. It shows that the bandpass response will have weaker stopband attenuation than the typical one as the capacitance value of C_1 and C_2 are fixed to a very small value of 100 fF. As discussed in the previous section, f_{chop} should be much higher (i.e., 4 kHz) than the 1/f noise corner frequency (i.e., ~400 Hz) of the IA for noise minimization. According to the *LC* resonant equation, the center frequency (f_{center}) of the bandpass filter equals to $1/2\pi(LC)^{1/2}$, the inductance value can be calculated to be 15.83 kHz, where $f_{center} = f_{chop}$ is set for fulfilling the frequency translation condition.

B. Filter Implementation and Analysis

Referring to Fig. 5 the RT-LPF based on the OTA-C ladder structure is realized. Thanks to the Nauta cell no common-mode feedback circuit is required. The overall CLF circuit consists of 2 grounding resistors (g_{m0} and g_{m6}) for realizing R_1 and R_2 in Fig. 3, 4 series capacitors (C_1 and C_2), and 2 gyrators **A** and **B** which are exploited to implement equivalently the inductors, L_1 and L_2, respectively. Considering the front stage of the RT-LPF before the buffer, the voltage transfer function (V_1 / V_{in}) is given by,

$$\frac{V_1}{V_{in}} = \frac{j\omega C_1 / g_{mOTA}}{1 + j\omega C_1 / g_{mOTA} - \omega^2 C_1 C_{L1} / g_{mOTA}^2} = \frac{j\omega / Q_F\omega_0}{1 + j\omega / Q_F\omega_0 - \omega^2 / \omega_0^2} \qquad (3)$$

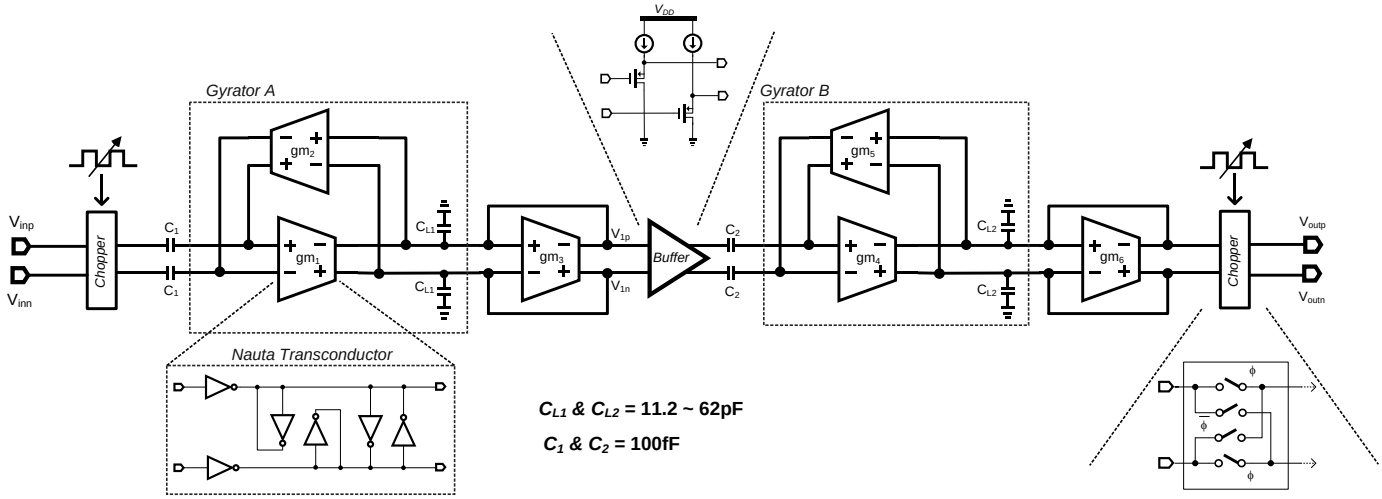

Fig. 5. Circuit implementation of a 2nd-order OTA-C RT-LPF.

by choosing $g_{mOTA} = g_{m1} = g_{m2}$, we obtain the filter parameters,

$$Q_F = \sqrt{\frac{C_{L1}}{C_1}} \quad \text{and} \quad \omega_0 = \frac{g_{mOTA}}{\sqrt{C_1 C_{L1}}} \tag{4}$$

where Q_F is the filter's quality factor and $f_{center} = 2\pi\omega_0$. Moreover, a source-follower buffer is added to separate the front and back stages of the RT-LPF, thus the loading effect to the gain of the front stage can be neglected and the transfer function of the 2nd-order bandpass filter (V_{out}/V_{in}) can simply be derived as (3).

Referring to (4) the bandwidth ($f_{passband}$) of the bandpass filter can be given by,

$$f_{passband} \approx \frac{\omega_0}{2\pi Q} = \frac{g_{mOTA}}{2\pi C_{L1}} \tag{5}$$

Eqs. (4) and (5) hint the way to control $f_{passband}$ without affecting the Q_F is by changing the OTA's transconductance (g_{mOTA}). This operation is equivalent to control the lowpass cutoff ($f_{cut\text{-}off}$) of the RT-LPF. However, since the input common-mode voltage of the OTA is fixed and the increment of g_{mP} and g_{mN} call for more power, adjusting g_{mOTA} to control $f_{passband}$ may not be that efficient. Thus, the cutoff tuning is achieved by changing the size of the gyrator's loading capacitors (C_{L1} and C_{L2}). Changing C_{L1} and C_{L2} will also alter f_{center} although the effect is less severe than using g_{mOTA}. As a result, the RT-LPF should include a variable clock signal generator to track f_{center} with f_{chop}, which is the key practical concern of this filter.

5. SIMULATION RESULTS

Theoretically the bandpass filter transfer gain at the central frequency is equal to unity, which is consistent to the simulation result of the passive model as shown in Fig. 4. However in the active realization, gain variation was observed as shown in Fig. 6, which is mainly due to the different in Q_F when the capacitance ratio between C_1, C_2 and C_{L1}, C_{L2} are

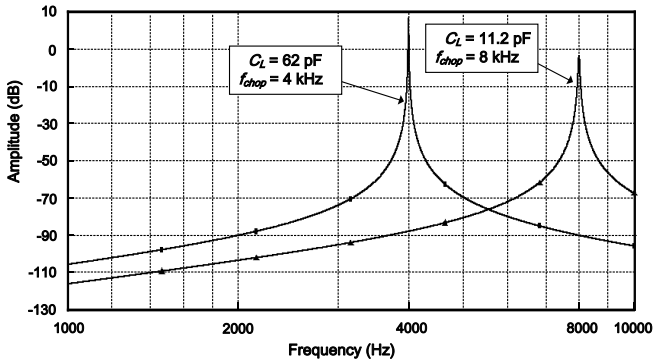

Fig. 6. Frequency responses of the bandpass OTA-C filter in Fig. 5 before chopper demodulation under two different sizes of C_L and f_{chop}.

varying in order to control $f_{passband}$. Figure 6 also demonstrates that when C_L and f_{chop} are set to 62 pF and 4 kHz respectively, the corresponding $f_{passband}$ is around 4 Hz with its center frequency equal to f_{chop}. Similarly, $f_{passband}$ will become 22.5 Hz when C_L and f_{chop} are changed to 11.2 pF and 8 kHz, respectively. Both of these configurations can be calculated by using the OTA transconductance, which is equal to 1.58 nV/A here. The tuning of the bandwidth is linear according to (5) if the parasitic capacitance of the gyrator is negligible.

The simulated response of the RT_LPF after chopper demodulation is shown in Fig. 7. The cutoff is not exactly half the $f_{passband}$ as the bandpass response is not the ideal shaping and the demodulated residual odd harmonic components may also affect the final lowpass response. However, the result shows that a proper lowpass response with -40 dB/decade stop-band attenuation can be obtained, providing that the bandpass filter quality factor is higher than 10, which is reasonable to achieve in practice. The maximum tuning range of the lowpass cutoff is around 15 Hz.

Figure 8 shows the simulated output noise power density of the RT-LPF before and after frequency translation. It can be observed that in Fig. 8(a) the maximum output noise is nearly

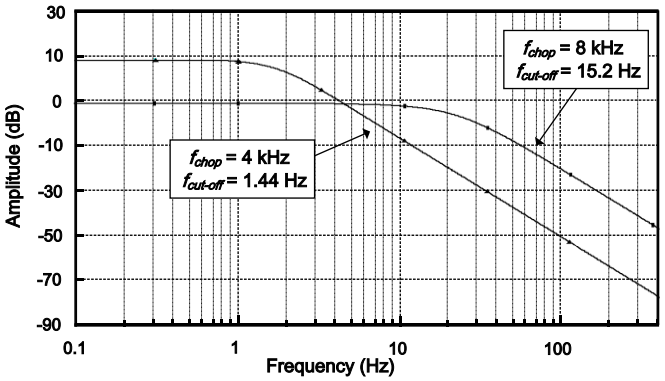

Fig. 7. Frequency responses of the RT-LPF after demodulation with different f_{chop} and $f_{cut\text{-}off}$.

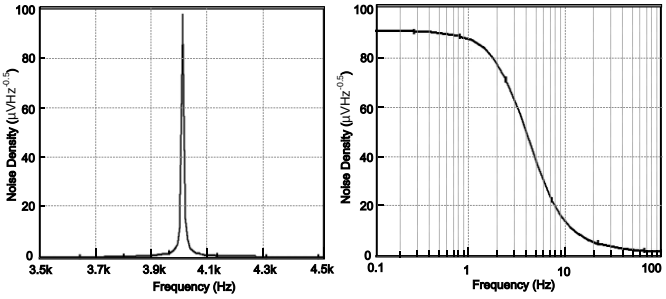

Fig. 8. Output noise-voltage density of the RT-LPF (a) before demodulation and (b) after demodulation when f_{chop} = 4 kHz.

100 μV/√Hz, which is mainly dominated by the *LC* resonant circuit components. After the signal was demodulated back to low frequency, the output noise due to the *LC* resonant remains in a certain level without further enhancement, as the 1/*f* noise has already been eliminated by the bandpass characteristic of the IA.

This design can be compared with a prior work [1] which uses a Bipolar-CMOS-DMOS technology to achieve a similar cutoff range. As listed in Table I, this work shows lower power consumption and smaller output noise due to the techniques of frequency translation and a more reasonable transconductance value based on the Nauta-cell OTA. On the other hand, the stopband attenuation in this work is fixed to –40 dB/decade without involving a resonant zero to limit the attenuation at high frequency as in [1]. Nevertheless, this work still shows less dynamic range than [1] due to the existence of chopper spikes. The dynamic range of the RT-LPF should be improved after the spike filter is adopted, as depicted in Fig. 1.

6. CONCLUSIONS

A chopper-stabilized response-translating lowpass filter (RT-LPF) is proposed. An ultra-low cutoff down to 1.4 Hz is achieved with a strong relaxation of time-constant by utilizing the frequency-translation property of the chopper stabilization, which has been the technique of 1/*f*-noise reduction, but is now extended to translate the bandpass filter characteristic of the IA to perform lowpass filtering. The implementation is further

Table I Performance benchmarks of the proposed RT-LPF and [1]

	This work (Simulation)	[1] (Experiment)
Technology	90 nm CMOS	0.35 μm Bipolar-CMOS-DMOS
Filter Order	Second-order	Second-order
Supply Voltage	3 V	3.3 V
Supply Current	8.37 μA*	50 -500 μA
Cut-off Frequency	1.44 – 15.2 Hz	1.5 – 15 Hz
Total Output Noise Amplitude (peak-to-peak)	88.28 μV/√Hz	900 μV/√Hz
DC Gain	-1 to 8 dB	0 dB
Dynamic Range	49.5 dB	60 dB

* — Excluding clock generator and backend filtering

optimized by using a power-and-area-efficient Nauta cell as the OTA. Simulation results show that the RT-LPF achieves 1.4-to-15-Hz cutoff tuning, –40 dB/decade stopband attenuation and 88.28 μV/√Hz output noise voltage density. The power consumption is 25.1 μW at a single 3-V supply.

ACKNOWLEDGMENT

This work is funded by the University of Macau Research Committee and Macau Science and Technology Development Fund (FDCT).

REFERENCES

[1] P. Bruschi, N. Nizza, F. Pieri, M. Schipani, D. Cardisciani"A Fully Integrated Single-Ended 1.5–15-Hz Low-Pass Filter With Linear Tuning Law" *IEEE J. Solid-State Circuits, vol. 42, No. 7, pp. 1522–1528*, Jul. 2007.

[2] S. Solis-Bustos, J. Silva-Martinez, F. Maloberti, and E. Sanchez-Sinencio, "A 60 dB Dynamic-Range CMOS Sixth-Order 2.4 Hz Low-Pass Filter for Medical Applications." *IEEE Trans. Circuits Syst. II, vol. 47, pp. 1391–1398,* 2000.

[3] Qian, Y. P. Xu and X. Li "A CMOS Continuous-Time Low-Pass Notch Filter for EEG Systems." in *Analog Integrated Circuits and Signal Processing*, Springer, *vol. 44, no.3, pp. 231–238,* Sep. 2005.

[4] C. C. Enz and G. C. Temes, "Circuit Techniques for Reducing the Effects of Opamp Imperfections: Autozeroing, Correlated Double Sampling, and Chopper stabilization," *Proc. IEEE, vol. 84, no. 11, pp. 1584–1614,* Nov. 1996.

[5] R. F. Yazicioglu, P. Merken, and P. Robert, "A 60 μW 60 nV/√Hz Readout Front-End for Portable Biopotential Acquisition Systems ," *IEEE J. of Solid-State Circuits, vol. 42, no. 5,* May 2007.

[6] Nauta, B., & Seevinck, E., "A CMOS Transconductance-C Filter Technique for Very High Frequency." *IEEE J. Solid-State Circuits*, vol. 27, pp. 142–153, 1992.